Occurrence of NO-reburning in MILD combustion evidenced via chemical kinetic modeling

André Nicolle, Philippe Dagaut *

Centre National de la Recherche Scientifique, Laboratoire de Combustion et Systèmes Réactifs, 1C, Avenue de la Recherche Scientifique, 45071 Orléans Cedex 2, France

Abstract

A numerical study of the diluted oxidation of CH_4 was performed to investigate the potential importance of the NO-reburning mechanism in conditions relevant to MILD combustion. It turns out that the NO–HCN conversion reactions are particularly active before auto-ignition. During this period, the nitrogen contained initially in NO is stored in HCN and NH_3. The extent of this phenomenon depends on the equivalence ratio and on the unmixedness. Subsequently, nitrogen is restored in its original NO form. In the post-ignition period, thermal and N_2O pathway to NO grow in importance. Therefore, this study revealed a sequential character of the nitrogen chemistry. Although these effects have both chemical and thermal origin, a transient NO-reburning mechanism was also evidenced via modeling at constant temperature demonstrating it is mainly related to the fuel-ignition chemistry.
© 2006 Elsevier Ltd. All rights reserved.

Keywords: NO_x; Flameless oxidation; Reburning

1. Introduction

Unlike conventional combustion, diluted combustion technologies enable engineers to increase thermal efficiency and simultaneously reduce nitrogen oxides (NO_x) emissions [1]. Despite the small concentration of oxygen in such combustion chambers, the Zel'dovich thermal-NO mechanism remains active in MILD conditions for long residence times [2–4]. Nevertheless, exhaust gas recirculation causes a decrease of the peak temperature, which reduces the importance of the thermal-NO and favors the N_2O route to NO [2,5].

NO reduction via reactions with hydrocarbon fragments called NO-reburning [6] is usually neglected in MILD conditions [4]. To our knowledge, very few kinetic studies of the importance of this mechanism have been undertaken in diluted combustion conditions [7,8]. However, the strong exhaust gas recirculation used in flameless combustion is responsible for the presence of nitrogen oxides in the reactive mixture. Nicolle [9] showed computationally that in plug flow conditions NO-reburning occurs during the auto-ignition of the reacting mixture. In a recent pilot-scale experimental study, Masson [10] observed that NO injected via exhaust gas recirculation is reduced in the flame region close to injection under MILD combustion. Therefore, it appears that NO can react with the injected fuel even in overall fuel-lean conditions.

De Joannon et al. [11] indicated that a storage process of methyl radicals in the C_2 recombination pathway takes place during the diluted combustion of methane. As the chain branching progresses, the C_2 compounds are oxidized into acetaldehyde which in turn dehydrogenates, yielding CH_3CO. CH_3 radicals are further produced through the thermal decomposition of CH_3CO. Since this oxidation mechanism leads to a transient increase of the concentration of CH_3, known to play a significant role in NO-reburning [12,13], it seems quite conceivable that the re-circulated nitrogen monoxide could be converted into HCN during the ignition period.

---

* Corresponding author. Tel.: +33 238 25 54 66; fax: +33 238 69 60 04.
  E-mail address: dagaut@cnrs-orleans.fr (P. Dagaut).

The aims of the present work are twofold: (i) to show the evolution of the importance of the NO consumption pathways as a function of the progress variable, (ii) to investigate the impact of the equivalence ratio, the unmixedness and the use of different kinetic schemes on these pathways.

2. Chemical kinetic modeling

Since diluted combustion proceeds in a combustion regime close to the distributed reactions regime [2], we may model this combustion using a perfectly-stirred reactor [1,14–16] or partially-stirred reactor [17] model. The PaSR model allows accounting for non-ideal micro-mixing in the combustion chamber. Cavaliere and de Joannon [18] showed that MILD combustion can also take place under plug-flow reactor (PFR) conditions; they named this combustion mode 'homogeneous flow flowing ignition'. Therefore, we also used the PF model which actually corresponds to a case of perfect unmixedness. These models allow using a detailed kinetic scheme for the oxidation of the fuel

and for the nitrogen oxides chemistry and therefore to efficiently probe the kinetic aspects of MILD combustion.

In the present modeling, we mainly used the unsteady PSR and PaSR models from the Chemkin 4.0 code [19]. The residence time in the reactor and its volume were, respectively, fixed to 100 ms and 50 cm^3. In all the computations, the combustion was supposed to proceed adiabatically (i.e. $Q_{loss} = 0$). In the PaSR calculations, the mixing process was described by a modified coalescence-redispersion model [20]. Using this widely used model, Chang and Chen [21] obtained NO concentration levels lying between those given by the IEM and LEM models. A value of 1 ms was chosen for the time step of the Monte Carlo simulation. We used 1000 stochastic particles in the PaSR calculations in order to correctly predict the statistics of the computed scalars [22]. For each time step [23], the program chooses 10 particles and set their properties to those of the inlet mixture. Then, some of the particles are randomly chosen and mixed. Finally, the mass and energy equations of a PSR are integrated over the time step for each of the 1000 particles.

Table 1
Selected reactions from the present chemical kinetic mechanism

Reaction	A	n	E	Note
169. $N_2 + O = N + NO$	$1.00E+14$	0.0	75490.0	(a)
170. $N + O_2 = NO + O$	$6.40E+09$	1.0	6280.0	(b)
171. $N + OH = NO + H$	$3.80E+13$	0.0	0.0	(c)
172. $NO + HO_2 = NO_2 + OH$	$2.10E+12$	0.0	−480.0	(d)
173. $NO_2 + H = NO + OH$	$1.00E+14$	0.0	362.0	(e)
176. $N_2O + M = N_2 + O + M$	$3.00E+14$	0.0	55500.0	(f)
Enhanced by 16.25 for H_2O, 1.875 for CO, 3.75 for CO_2, 16.25 for CH_4, 16.25 for C_2H_6				
181. $NH + OH = NO + H_2$	$2.00E+13$	0.0	0.0	(g)
184. $NH + NO = N_2O + H$	$4.30E+14$	−0.5	0.0	(h)
188. $NH_3 + OH = NH_2 + H_2O$	$2.04E+06$	2.0	566.0	(b)
189. $NNH + M = N_2 + H + M$	$2.00E+14$	0.0	20000.0	(i)
Enhanced by 16.25 for H_2O, 1.875 for CO, 3.75 for CO_2, 16.25 for CH_4, 16.25 for C_2H_6				
190. $NNH + O = NH + NO$	$5.00E+13$	0.0	0.0	(j)
213. $CH_3 + NO = HCN + H_2O$	$1.50E−01$	3.5	3950.0	(j)
229. $HCCO + NO = HCNO + CO$	$3.34E+13$	0.0	700.0	(k)
230. $HCCO + NO = HCN + CO_2$	$8.99E+12$	0.0	700.0	(k)
233. $CH_3O_2 + NO = CH_3O + NO_2$	$2.11E+12$	0.0	−358.0	(l)
239. $HNCO + H = NH_2 + CO$	$2.20E+07$	1.7	3800.0	(m)
245. $HCN + O = NCO + H$	$1.38E+04$	2.6	4980.0	(n)
252. $NCO + H = NH + CO$	$5.00E+13$	0.0	0.0	(b)

Note: $k = A \cdot T^n \cdot \exp(-E/RT)$; A units mol, cm, s, and K, E units cal/mol. (a) Michael JV, Lim KP. Rate constants for the N_2O reaction system: thermal decomposition of N_2O; $N + NO = N_2 + O$; and implications for $O + N_2 = NO + N$. J Chem Phys 1992;97:3228–34; (b) Miller JA, Bowman CT. Mechanism and modeling of nitrogen chemistry in combustion. Prog Energ Combust Sci 1989;15:287–338; (c) Baulch DL, Cobos CJ, Cox RA, Frank P, Hayman G, Just Th, et al. Evaluated kinetic data for combustion modelling. J Phys Chem Ref Data 1994;23(Suppl. I):847–1033; (d) Lightfoot PD, Cox RA, Crowley JN, Destriau M, Hayman GD, Jenkin ME, et al. Organic peroxy radicals: kinetics, spectroscopy and tropospheric chemistry. Atmos Environ Part A 1992;26:1805–961; (e) Ko T, Fontijn A. High-temperature photochemistry kinetics study of the reaction $H + NO_2 = OH + NO$ from 296 to 760 K. J Phys Chem 1991;95:3984–87; (f) Michael JV, Lim KP. Rate constants for the N_2O reaction system: thermal decomposition of N_2O; $N + NO = N_2 + O$; and implications for $O + N_2 = NO + N$. J Chem Phys 1992;97:3228–34; (g) Cohen N, Westberg KR. Chemical kinetic data sheets for high-temperature reactions. Part II. J Phys Chem Ref Data 1991;20:1211–311; (h) Miller JA, Smooke MD, Green RM, Kee RJ. Combust Sci Technol 1983;34:149–76; (i) Branch MC, Kee RJ, Miller JA. Combust Sci Technol 1982;29:147–65; (j) Glarborg P, Alzueta MU, Dam-Johansen K, Miller JA. Kinetic modeling of hydrocarbon/nitric oxide interactions in a flow reactor. Combust Flame 1998;115:1–27; (k) Dagaut P, Lecomte F, Chevailler S, Cathonnet M. Mutual sensitization of the oxidation of nitric oxide and simple fuels over an extended temperature range: experimental and detailed kinetic modeling. Combust Sci Tech 1999;148:27–57; (l) Baulch DL, Cobos CJ, Cox RA, Esser C, Frank P, Just Th, et al. Evaluated kinetic data for combustion modeling. J Phys Chem Ref Data 1992;21:411–29; (m) Miller JA, Melius CF. A theoretical analysis of the reaction between hydrogen atoms and isocyanic acid. Int J Chem Kinet 1992;24:421–32; (n) Glarborg P, Miller JA. Mechanism and modeling of hydrogen cyanide oxidation in a flow reactor. Combust Flame 1994;99:475–83.

The kinetic scheme used in this work is a skeletal mechanism derived from the detailed scheme of [24]. It involves only 95 species and 265 reactions. It was validated against a wide range of conditions: premixed flames, flow reactors, and shock tube. It includes both low- and high-temperature combustion chemistry. A subset of this scheme is given in Table 1. The pressure-dependencies of unimolecular reactions and of some pressure-dependent bimolecular reactions were taken into account. The rate constant for the reverse reactions were computed from the forward ones and the equilibrium constants calculated using thermochemical data [23]. Fig. 1 presents several examples of the mechanism validation.

In the present computations, the exhaust gas recirculation was implicitly taken into account by including CO_2, H_2O and NO in the reacting mixture. Table 2 summarizes the conditions chosen for our simulations. N_2 was chosen as bath gas. The amount of oxygen contained in CO_2, H_2O and NO was not taken into account in the determination of the equivalence ratio, φ. Cavaliere's and Peters' criteria [1,15] are met since the difference between the temperature extrema remains lower than 25% of the initial temperature. Thus, these conditions are representative of flameless combustion.

Table 2
Initial conditions for the numerical simulations

Model	T_{in} (K)	P (atm)	t (ms)	$CH_{4,in}$	$O_{2,in}$	H_2O_{in}	NO_{in} (ppmv)
PSR, PaSR, or PFR	1400	1	100	1.5% vol	3% vol/φ	20% vol	100

3. Results and discussion

A first simulation was performed under stoichiometric conditions. The main results of the computations are given in Fig. 2. It revealed that the inlet NO is partially consumed before auto-ignition of the mixture (i.e. <30 ms). Reaction rate analyses showed that NO is converted into HCN and NH_3 through the pathway $NO \rightarrow HCN \rightarrow NCO \rightarrow HNCO \rightarrow NH_2 \rightarrow NH_3$. Very early, the reaction (213) converts NO into HCN. At longer time, the reaction (230) takes over, dominating the NO–HCN conversion close to ignition.

$$CH_3 + NO = HCN + H_2O \quad (213)$$

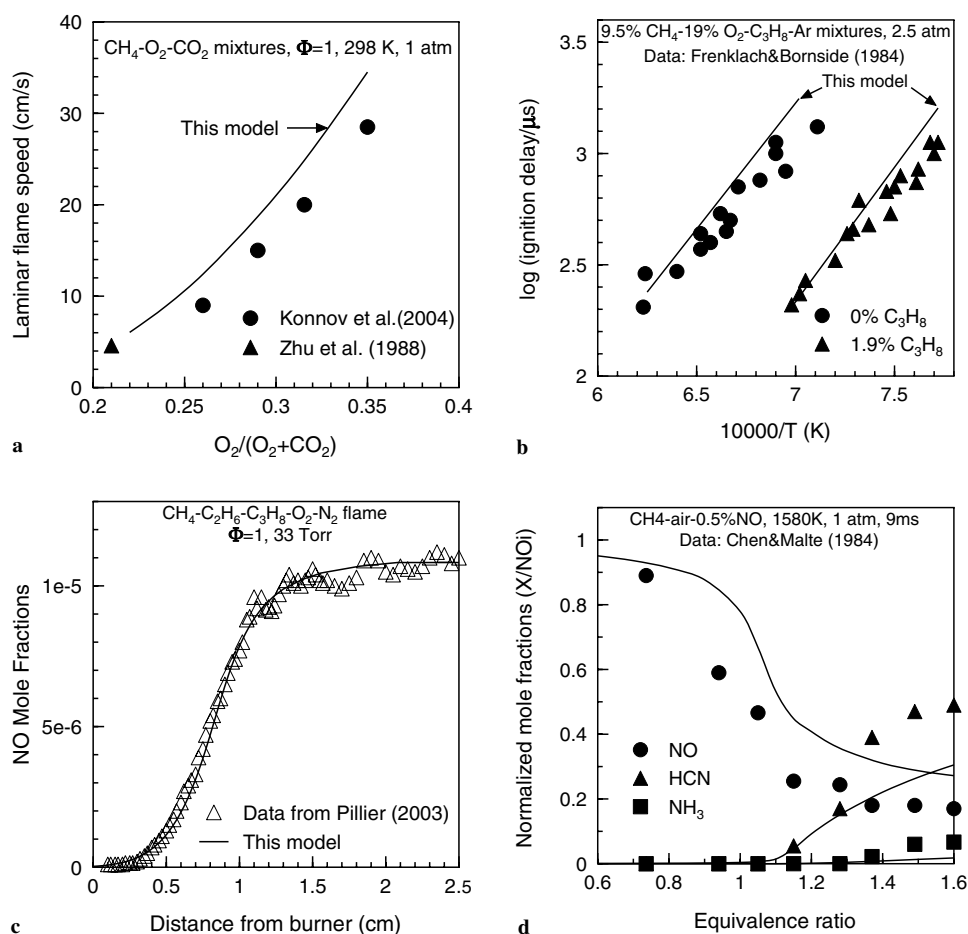$$HCCO + NO = HCN + CO_2 \quad (230)$$

Fig. 1. Validation of the present kinetic scheme (lines) against experimental data (symbols) taken from [25–29].
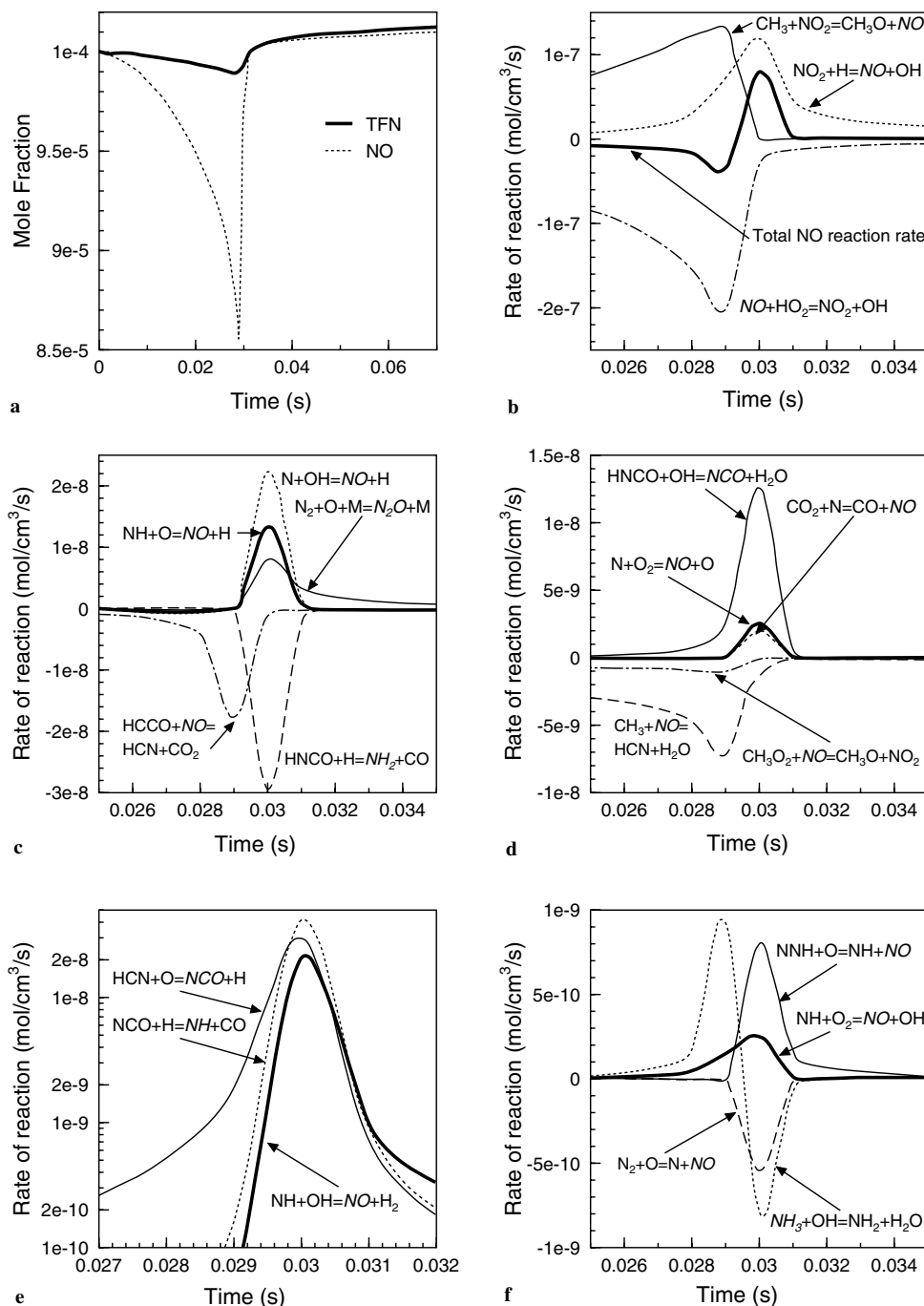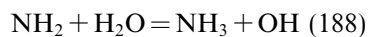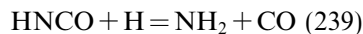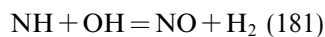
Fig. 2. Species and rates of reaction profiles plotted against time for the simulation of a stoichiometric combustion using the PSR model. Initial conditions: 1.5% CH_4 + 3% O_2 + 10% CO_2 + 20% H_2O + 100 ppmv NO + N_2. TFN represents the sum of the mole fractions of NO, HCN, HNCO, HCNO, and NH_3. The reaction rates refer to the species in italic.

The oxidation of HCN was shown to produce ammonia via the sequence of reactions:

$$HCN + O = NCO + H \quad (245)$$

$$NCO + H_2O = HNCO + OH \quad (240)$$

$$HNCO + H = NH_2 + CO \quad (239)$$

$$NH_2 + H_2O = NH_3 + OH \quad (188)$$

In turn HCN and NH_3 were converted into NO via the sequence of reactions:

$$HCN + O = NCO + H \quad (245)$$

$$NCO + H = NH + CO \quad (252)$$

$$NH + O = NO + H \quad (183)$$

$$NH + OH = NO + H_2 \quad (181)$$

and

$$NH_3 + OH = NH_2 + H_2O \quad (188)$$

$$NH_2 + OH = NH + H_2O \quad (185)$$
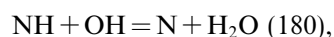
$$NH_2 + H = NH + H_2 \quad (186)$$

Fig. 2 shows that the rate of reaction (−188) changes of sign, from positive to negative, just before auto-ignition, indicating that it successively forms and consumes NH_3. The sequence of reactions (245) followed by reaction (252) and reaction (181) yields NO. During the ignition period, the NNH and prompt-NO pathways also contribute to the formation of NO. Their contribution remains of secondary importance because of the high concentration of steam (20% vol.) that inhibits both pathways [9,30]. The initial water concentration has clearly an influence on the HCN → NO oxidation since water addition is known to induce the depletion of O radicals [2,31]. Actually, previous kinetic studies of the oxidation of HCN showed that the reactions with OH are important in presence of steam [32] whereas in absence of water vapor, HCN mostly oxidizes by reaction with O-atoms [33]. Finally, after ignition, NO increases slowly with time. During this period, we note the increased importance of the thermal and N_2O routes to NO. These results are consistent with those obtained previously in plug flow conditions [9]. It should be noted that this sequential character of the nitrogen chemistry still appears under constant-temperature conditions.

3.1. Influence of the equivalence ratio

In this section, we describe the effect of the equivalence ratio on the nitrogen chemistry by varying the inlet O_2 mole fraction and keeping constant the initial carbon mole fraction. In order to interpret the computed temporal profiles, we define an adimensioned time as the ratio of the elapsed time to the auto-ignition delay (corresponding to the inflection point of the temporal profile of the temperature). As expected, the extent of reburning is increased by increasing the equivalence ratio of the initial mixture (Fig. 3). Beyond a given equivalence ratio, a second reburning phenomenon occurs. For equivalence ratios greater than 1.5, the computations showed the NO mole fraction decreases monotonously with time. According to the model, the NO-reburning mechanism has an indirect impact on the thermal-NO pathway. Indeed, Fig. 4 shows that the asymptotic mole fraction of the N radical increases if the inlet mixture becomes more fuel-rich due to the increased production of the N atom. The model indicated the following sequence of reactions associated with the intermediate formation of HCN through the NO-reburning mechanism is responsible for this phenomenon:

$$HCN + O = NH + CO \quad (246)$$

$$HCN + O = NCO + H \quad (245)$$

$$NCO + H = NH + CO \quad (252)$$

$$NH + H = N + H_2 \quad (182)$$

$$NH + OH = N + H_2O \quad (180),$$

followed by $N + OH = NO + H$ (171) and $N + O_2 = NO + O$ (170).

Conversely, the OH asymptotic mole fraction decreases with increasing equivalence ratio. This is partly due to the reduction of the final temperature. Indeed, Fig. 5 shows that the isolated kinetic effect of the equivalence ratio variation is qualitatively similar to the overall thermokinetic effect even if the global effect on the temporal OH mole fraction profile is much more complex due to discrepancies in the ignition delay.

Therefore, the variation of the net rate of reaction 171 as a function of the equivalence ratio and the progress of the combustion is impacted in a complex way, as depicted in Fig. 4.
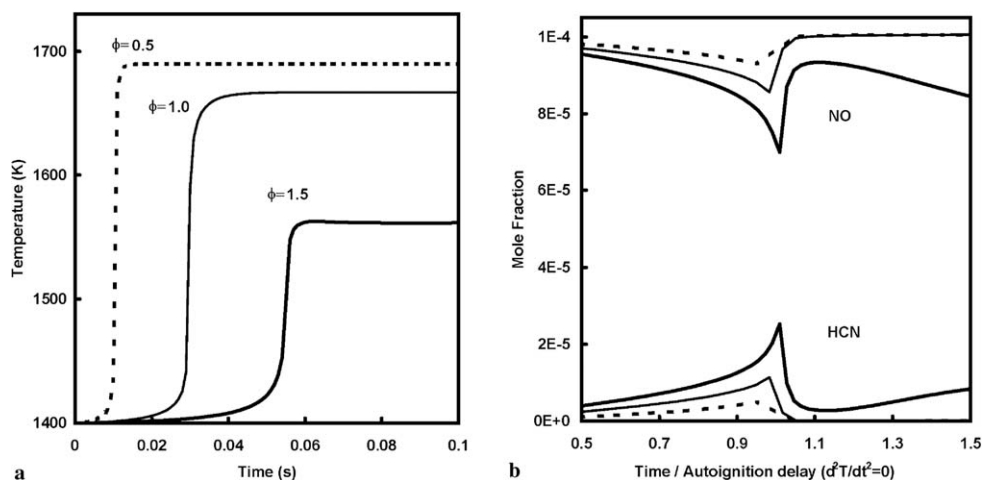

Fig. 3. Influence of the equivalence ratio ($\varphi = 0.5$, 1 and 1.5) on the temporal profiles of temperature and mole fractions of NO and HCN in PSR configuration.
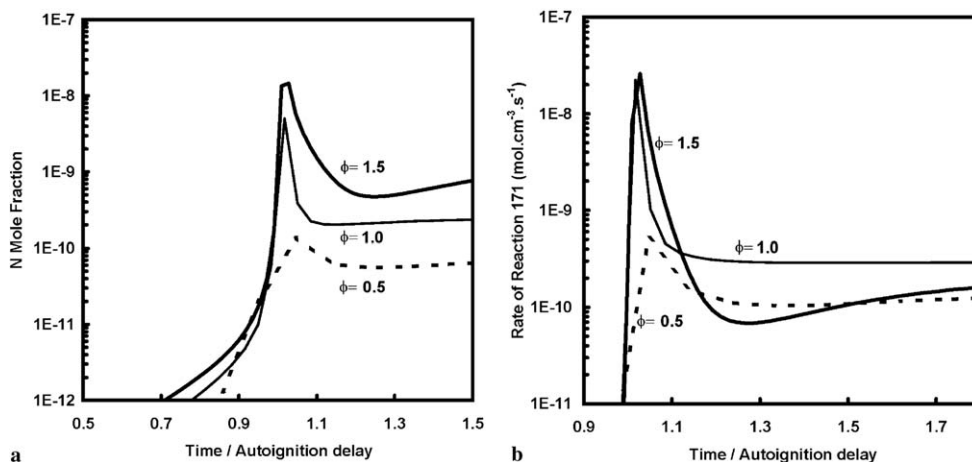
Fig. 4. Influence of the equivalence ratio on the mole fraction of N-atoms and on the rate of reaction $N + OH = NO + H$ (171) in PSR configuration.
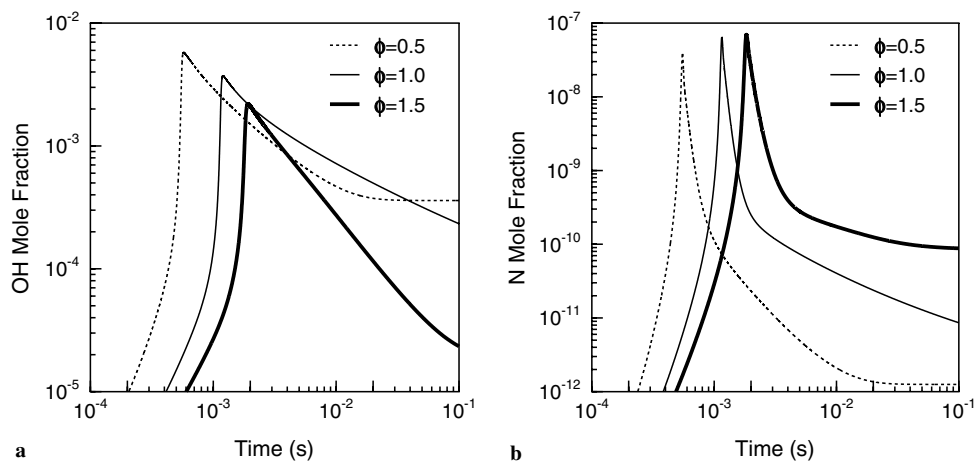

Fig. 5. Influence of the equivalence ratio ($\varphi = 0.5$, 1 and 1.5) on the OH and N mole fraction profiles in isothermal plug flow configuration at 1686 K.

3.2. Impact of the unmixedness

In this section, we describe the effect of the unmixedness on the nitrogen chemistry by varying the mixing time from 0 to 50 ms, at $\varphi = 1$. The ratio of the mixing time and the auto-ignition delay ranges from 0 to 1.8, whereas the ratio of the mixing and the residence times ranges from 0 to 0.5 and the unmixedness ranges from 0 to 0.6.
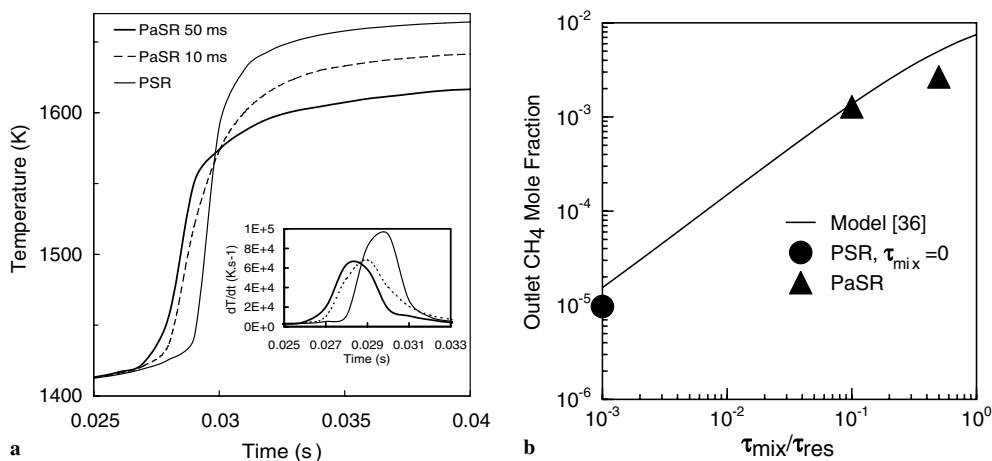

Fig. 6. Influence of mixedness on the temperature and fuel conversion. (a) The mixing time varies from 0 to 50 ms; (b) comparison between the model of [36], PaSR calculations ($\varphi = 1$) and PSR modeling ($\varphi = 1$, $\tau_{mix} = 0$). τ_{mix} and τ_{res} represent, respectively, the mixing and residence times.

Fig. 6 presents the influence of the mixing time on the temperature profile. We note that the mixing time has a significant influence on the auto-ignition delay time. Our results agree qualitatively with those obtained by Correa and Dean [34] for the auto-ignition of lean *n*-heptane/air mixtures using an initial temperature of 1000 K. They explained the diminution of the auto-ignition delay with the increase of the unmixedness arguing that the rich particles lead the ignition process because of their intrinsic shorter ignition delays, in agreement with [23]. Our study also shows that the effect of mixing time on the ignition delay becomes less discernible at large mixing times. These results are of capital importance for the understanding of the MILD combustion regime since it can be considered as a continuous auto-ignition [1].

The peak value of the derivative dT/dt decreases if the mixedness diminishes (Fig. 6). This result is similar to that obtained [35] for the combustion of methane. Moreover, Fig. 6 shows that the unmixedness also has a strong impact on the final mole fraction of methane. Our calculations agree well with the asymptotic value $(\tau_{mix}[CH_4]_{in})/(\tau_{mix} + \tau_{res})$ of Balakotaiah's model [36].

Fig. 7 presents the effect of mixedness on the NO profiles. As can be seen from this figure, the extent of NO reduction varies significantly with the mixing time and seems to reach a minimum for intermediate mixing times. Reaction rate analyses indicate that this phenomenon originates from the effect of mixing time on the CH_3 concentration profile. Indeed, Fig. 8 shows that the peak mole fraction of CH_3 reaches a minimum with respect to the mixing time (2.33×10^{-4}, 2.0×10^{-4}, 2.6×10^{-4} at mixing times of, respectively, 0, 10, and 50 ms) whereas that of HCCO in increases in the same range of mixing times (4×10^{-7}, 5.6×10^{-7}, 15.4×10^{-7} at mixing times of, respectively, 0, 10, and 50 ms). As can be seen from Fig. 9, the rate of reaction 213 reaches similarly a minimum. This trend was also observed for the acetylene mole fraction profile. Conversely, the peak mole fraction of CH, CH_2 and HCCO increase with the mixing time, which implies that the rates of their reactions with NO during auto-ignition also increase. The asymptotic behavior of NO mole fraction profile is mainly related to thermal effects since the unmixedness results in a smaller temperature rise during the ignition. Consequently, an increase in the mixing time
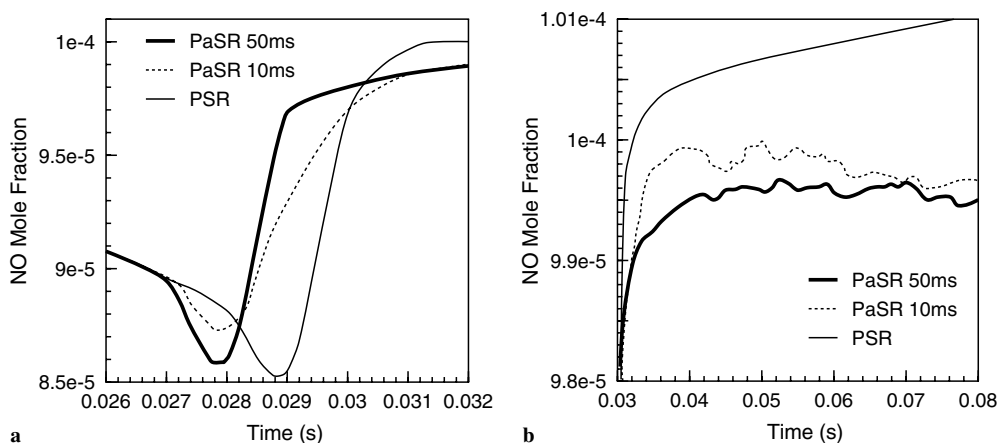

Fig. 7. Influence of mixedness on the NO mole fraction profile. The mixing time varies from 0 to 50 ms.
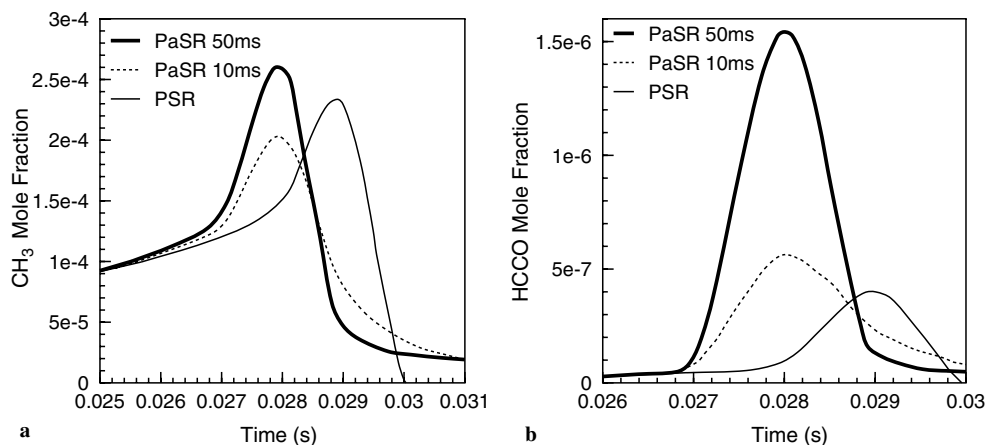

Fig. 8. Influence of mixedness on the mole fraction profiles of CH_3 and HCCO. The mixing time varies from 0 to 50 ms.
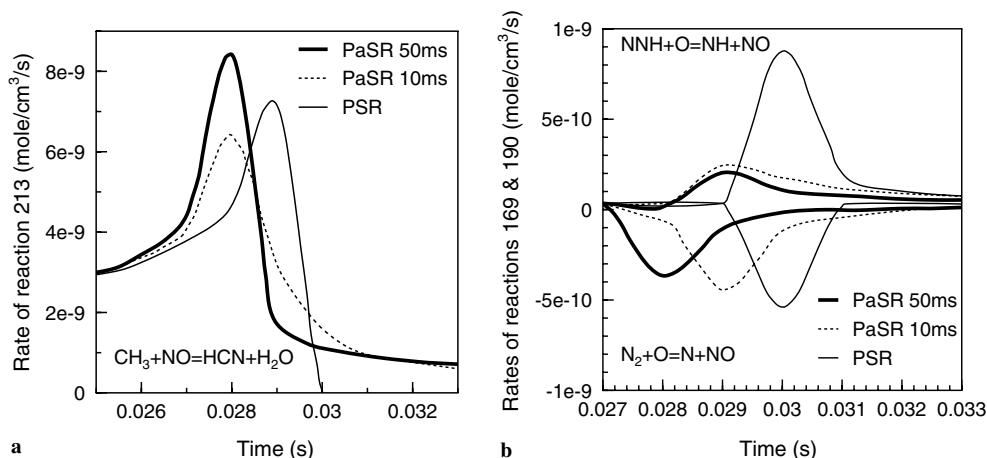
Fig. 9. Influence of mixedness on the rates of reactions $CH_3 + NO = HCN + H_2O$ (213), $N_2 + O = N + NO$ (169) and $NNH + O = NH + NO$ (190).

contributes to hinder the Zel'dovich and the NNH pathways to NO since the post-ignition concentrations of O and OH strongly decrease with the mixing time. In agreement with [37], the net rate of reaction 169 remains negative but its absolute value becomes smaller due to the depletion of N radicals at large mixing times.
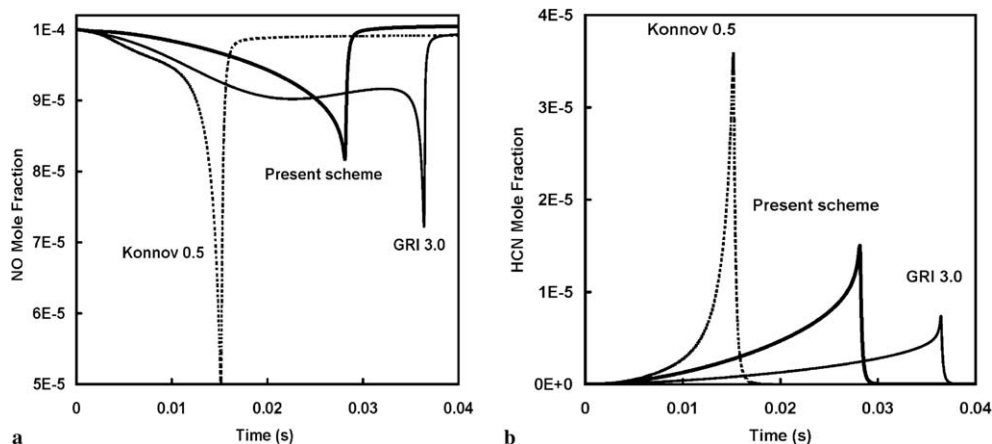

Fig. 10. Influence of the kinetic scheme used [40,42] on the computed mole fraction profiles obtained using the PFR model ($\varphi = 1$).
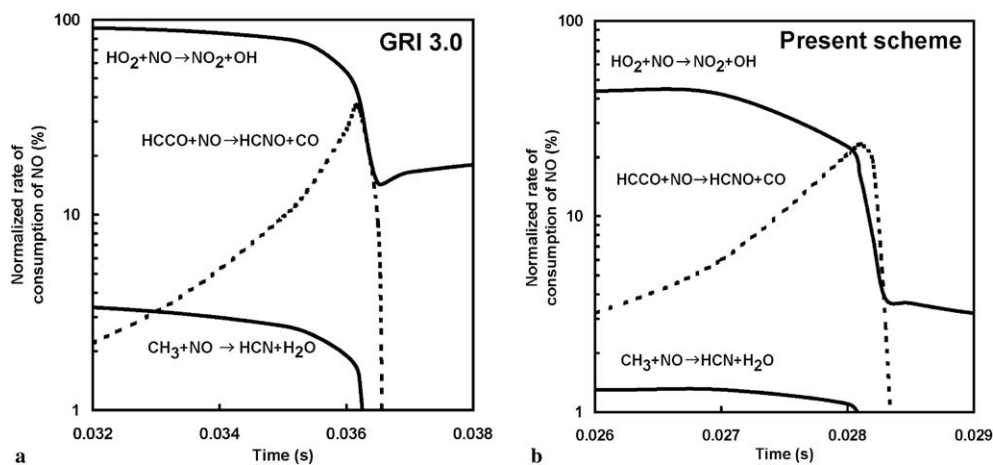

Fig. 11. Comparison of the temporal behavior of the main NO removal pathways using the PFR model ($\varphi = 1$) and the kinetic schemes from [42] (a) and this work (b).

3.3. Influence of the kinetic scheme

In this section, we compare the predictions obtained using several mechanisms from the literature to ensure that the reburning phenomenon is not only predicted by our kinetic scheme. The calculations were carried out in plug flow conditions (PFR) using the Senkin code [38] at an equivalence ratio of one. The results were post-processed using the KinalC and Mechmod codes [39]. Fig. 10 presents the mole fraction profiles obtained using the present kinetic scheme and two literature kinetic mechanisms [40,42]. These models predict a final temperature close to 1686 K, the mutual differences being smaller than 1 K. Although our scheme predicts an intermediate auto-ignition delay, the predicted NO-reburning is weaker than obtained with the other mechanisms. The strong conversion predicted by [40] was expected since this mechanism over-predicts the NO-reburning in plug flow experiments [41]. The profile obtained using [42] exhibits a complex behavior before auto-ignition even if NO-reburning clearly occurs. Indeed, NO is first converted into NO_2; the NO_2 mole fraction peaks at 8 ppmv for $t = 20$ ms. Subsequently, NO_2 yields NO while the reburning mechanism converts NO into HCN. The peak mole fraction of HCN predicted by [42] seems small in comparison with the simultaneous strong consumption of if NO. Actually, as previously observed [43], the GRI Mech predicts a significant part of NO is converted into NH_3 yielding up to 4 ppmv of NH_3 are formed during the auto-ignition. Once again, this trend could be expected since GRI Mech over-predicts the NH_3 mole fraction in the experiments of [29]. Nevertheless, Fig. 11 demonstrates the similarity between the main NO removal pathways for two of the mechanisms. The main difference between GRI 3.0 and the present mechanism lies in the importance of the reaction $CH_3 + NO(+M) = CH_3\text{-}NO(+M)$ before ignition. This reaction is not included in the GRI Mech scheme, which explains the discrepancy between the two schemes for the contribution of the reaction $HO_2 + NO = NO_2 + OH$. To sum up, whatever the mechanism is, reaction 213 is active long before reaction 229 because of the early formation of CH_3. Since HCCO is only formed just before ignition via to the oxidation of the C_2 compounds, the contributions of reactions 229 and 230 exhibit a sharp rise there, contributing to a rapid conversion of NO into HCN.

4. Conclusion

The present kinetic modeling study of the oxidation of methane revealed the sequential character of the nitrogen chemistry in MILD conditions. According to the model, the NO–HCN, NH_3 conversion reactions are particularly active before auto-ignition. Subsequent oxidation processes recycle NO. The modeling showed that the extent of this phenomenon depends on the equivalence ratio and on the unmixedness. During the ignition period, NO formation via the NNH and prompt-NO mechanisms occur even if their contribution to the global formation of NO is of secondary importance. After ignition, the thermal and N_2O pathway to NO grow in importance whereas NO-reburning may also take place for fuel-rich mixtures. Although these processes have both chemical and thermal origin, the prediction of a transient NO-reburning mechanism from constant temperature simulations indicates it is mainly related to the fuel-ignition chemistry. Research is on-going to evaluate the chemical effect of water and carbon dioxide on the nitrogen chemistry during MILD combustion.

References

[1] Cavaliere A, de Joannon M. Prog Energy Combust Sci 2004;30: 329–66.
[2] Tabacco D, Innarella C, Bruno C. Combust Sci Tech 2002;174:1–35.
[3] Ju Y, Niioka T. Combust Theory Model 1997;1:243–58.
[4] Mancini M, Weber R, Bollettini U. Proc Combust Inst 2002;29: 1155–63.
[5] Yang W, Blasiak W. Fuel Process Technol 2005;86:943–57.
[6] Wendt JOL, Sterling CV, Matovich MA. Proc Combust Inst 1972;14:897–904.
[7] Sohn CH, Jeong IM, Chung SH. Combust Flame 2002;130:83–93.
[8] Fuse R, Kobayashi H, Ju Y, Maruta K, Niioka T. Int J Thermal Sci 2002;41:693–8.
[9] Nicolle A. Experimental and modeling study of the kinetics of flameless combustion. Doctoral Thesis. University of Orleans; 2005 [in French].
[10] Masson E. Experimental study of scalar and dynamic fields of flameless combustion. Doctoral Thesis. INSA Rouen; 2005 [in French].
[11] De Joannon M, Sabia P, Tregrossi A, Cavaliere A. Combust Sci Tech 2004;176:769–83.
[12] Miller JA, Durant JL, Glarborg P. Proc Combust Inst 1998;27: 235–43.
[13] Kolb T, Jansohn P, Leuckel W. Proc Combust Inst 1988;22:1193–203.
[14] Plessing T, Peters N, Wünning JG. Proc Combust Inst 1998;27: 3197–204.
[15] Oberlack M, Arlitt R, Peters N. Combust Theory Model 2000;4: 495–509.
[16] Tsuji H, Gupta AK, Hasegawa T, Katsuki M, Kishimoto K, Morita M. High temperature air combustion: from energy conservation to pollution reduction. Boca Raton, FL: CRC Press LLC; 2003.
[17] Schütz H, Lueckerath R, Kretschmer T, Noll B, Aigner M. In: Eighth international conference on energy for a clean environment, Lisbon; 2005.
[18] Cavaliere A, de Joannon M. In: Proc European combust meeting, Louvain La Neuve; 2005.
[19] Kee RJ, Rupley FM, Miller JA, Coltrin ME, Grcar JF, Meeks E, et al. CHEMKIN Release 4.0, Reaction Design, Inc., San Diego, CA; 2004.
[20] Janicka J, Kolbe W, Kollmann W. J Non-equil Thermody 1979;4: 47–66.
[21] Chang WC, Chen JY. Proc Combust Inst 1996;26:2223–9.
[22] Sabel'nikov VA, Figueira Da Silva LF. Combust Flame 2002;129: 164–78.
[23] Chen JY. Combust Sci Tech 1997;122:63–94.
[24] Dagaut P, Nicolle A. Combust Flame 2005;140:161–71.

[25] Dyakov IV, Konnov AA, De Ruyck J. Khimicheskaya Fizika 2004;23:19–24.
[26] Zhu DL, Egolfopoulos FN, Law CK. Proc Combust Inst 1988;22:1537–45.
[27] Frenklach M, Bornside DE. Combust Flame 1984;56:1–27.
[28] Pillier L. Doctoral Thesis. University of Lille I; 2003 [in French].
[29] Chen AT, Malte PC. Western States Section of the Combustion Institute. The Combustion Institute, 23 October 1984, Stanford, CA, paper WSS/CI 84–86.
[30] Zhao D, Yamashita H, Kitagawa K, Arai N, Furuhata T. Combust Flame 2002;130:352–60.
[31] Shoji M, Yamamoto T, Tanno S, Aoki H, Miura T. Energy 2005;30: 337–45.
[32] Glarborg P, Miller JA. Combust Flame 1994;99:475–83.
[33] Dagaut P, Lecomte F, Chevailler S, Cathonnet M. Combust Sci Tech 2000;155:105–27.
[34] Correa SM, Dean AJ. Proc Combust Inst 1994;25:1293–9.
[35] Kraft M, Fey H, Schlegel A, Chen JY, Bockhorn H. A numerical study on the influence of mixing intensity on NO_x formation.

[36] Workshop on modelling of chemical reaction systems, Heidelberg; 1996.
[36] Balakotaiah V, Chakraborty S. Chem Eng Educ 2002;36(4):250–7.
[37] Choi GM, Katsuki M. Proc Combust Inst 2002;29:1165–71.
[38] Lutz AE, Kee RJ, Miller JA. SAND87-8248 Report, Sandia National Laboratories; 1987.
[39] Turanyi T. KINAL: a program package for kinetic analysis of reaction mechanisms. Comput Chem 1990;14:253–4.
[40] Konnov AA. A detailed reaction mechanism for small hydrocarbons combustion. Release 0.5. 2000. Available from: <http://home-pages.vub.ac.be/~akonnov/>.
[41] Alzueta MU, Glarborg P, Dam-Johansen K. Combust Flame 1997;109:25–36.
[42] Smith GP, Golden DM, Frenklach M, Moriarty NW, Eiteneer B, Goldenberg M, et al. GRI Mech 3.0. 1999. Available from: <www.me.berkeley.edu/gri_mech/>.
[43] Dagaut P, Luche J, Cathonnet M. Proc Combust Inst 2000;28: 2459–65.